Thin-Walled Structures 139 (2019) 372–388

Contents lists available at ScienceDirect

Thin-Walled Structures

journal homepage: www.elsevier.com/locate/tws

Full length article

Application of structural topology optimisation in aluminium cross-sectional design

Konstantinos Daniel Tsavdaridis[a,*], Evangelos Efthymiou[b], Alikem Adugu[c], Jack A. Hughes[d], Lukas Grekavicius[e]

[a] School of Civil Engineering, University of Leeds, Woodhouse Lane, LS2 9JT Leeds, UK
[b] Institute of Metal Structures, Department of Civil Engineering, Aristotle University of Thessaloniki, Thessaloniki, Greece
[c] WSP, 3 White Rose Office Park, Millshaw Park Lane, LS11 0DL Leeds, UK
[d] Robert Bird Group, 47-51 Great Suffolk St, SE1 0BS London, UK
[e] Cundall, Regent Farm Rd, Newcastle upon Tyne, NE3 3AF Newcastle, UK

ARTICLE INFO

Keywords:
Structural topology optimisation
Heuristic optimisation
SIMP technique
Extrusion
Aluminium profiles
Cross-section classification
Eurocode 9

ABSTRACT

Aluminium is lightweight and corrosion-resistant; however, its low Young's Modulus predisposes the need for better material distribution across its section to increase stiffness. This paper studies a holistic design optimisation approach with the power of structural topology optimisation aiming to develop novel structural aluminium beam and column profiles. The optimisation methodology includes forty standard loading combinations while the optimisation results were combined through an X-ray overlay technique. This design optimisation approach is referred here to as the Sectional Optimisation Method (SOM). SOM is supported by engineering intuition as well as the collaboration of 2D and 3D approaches with a focus on post-processing and manufacturability through a morphogenesis process. Ten optimised cross-sectional profiles for beams and columns are presented. The shape of one of the best performing optimised sections was simplified by providing cross-section elements with a uniform thickness and using curved elements of constant radius. A second level heuristic shape optimisation was done by creating new section shapes based on the original optimised design. The paper also carries out stub column tests using finite element analysis (FEA) to determine the loacl buckling behaviour of the above-optimised aluminium profiles under compression and to investigate the effectiveness of using the existing classification methods according to codified provisions of Eurocode 9. The herein presented work aims to integrate topology optimisation aspects in cross-sectional design of aluminium alloy element building applications, providing thus a new concept in design procedures of lightweight aluminium structures.

1. Background

1.1. Structural topology optimisation

Structural optimisation is a mathematical approach towards reducing the number of materials and hence cost while sustaining the applied loads. The application of structural optimisation has been effectively used in the fields of automotive and aerospace engineering to attain lightweight mechanical products [43]. Later, it was attempted in civil/structural engineering applications with the realisation that the materials are limited, thus it is necessary to save materials for a sustainable approach [2]. Structural topology optimisation gives the benefits of removing the material without compromising the performance of the member.

Structural optimisation problems are generally expressed by the following mathematical form [10]:

Structural Optimisation

$$\begin{cases} minimises/maximises\ f(x,\ y)\ with\ respect\ to\ x\ and\ y \\ \quad subject\ to \begin{cases} behavioural\ constraints\ on\ y \\ design\ constraints\ on\ x \\ equilibrium\ constraints. \end{cases} \end{cases}$$

where:

$f(x, y)$ – Objective function is a function used to classify design. For a design problem, one aims to either minimise or maximise the value and it usually measures weight, displacement or stress.

* Corresponding author.
E-mail address: k.tsavdaridis@leeds.ac.uk (K.D. Tsavdaridis).

https://doi.org/10.1016/j.tws.2019.02.038
Received 13 September 2018; Received in revised form 20 February 2019; Accepted 28 February 2019
Available online 20 March 2019

x – Design variable is a function or a vector that describes geometric or material properties of the design. The design variable can be changed during the optimisation process.
y – State variable is a function or a vector that describes the response of the structure, for a value of x.

It is an expression of an optimisation model, where a minimum or maximum value of an objective function (e.g., a performance measure of a structure) is being pursued/estimated while subjected to specific constraints and a design variable. The objective functions have many solutions due to their non-linearity. Therefore, they have multiple local minima, but only one global minimum, which is the main aim of design optimisation [3].

Structural optimisation can be separated into three main categories: size, shape, and topology optimisation [5]. Some overlaps between the three categories exist. For instance, shape optimisation could be considered a subclass of topology optimisation, but they are based on different techniques in terms of practical implementations. However, topology optimisation is the most popular and has proven to be the most effective as the number of openings (material free) do not need to be specified prior to the procedure and the structural forms are simply carved from a block of material.

There are numerous topology optimisation techniques available in the literature. The potential for the use of the Solid Isotropic Material with Penalisation (SIMP) interpolation scheme and the Variable Density Method (VDM) algorithms for non-linear optimisation is discussed herein.

SIMP is a micro approach based on varying the density of the material within a domain in finite element (FE) parts, as it is the most efficient and popular method for topology optimisation of linear elastic structures [34]. The procedure is based on performing FE analyses on the shape and then optimising the density of each element. The domain, loads, and constraints of the structure are specified and analysis is performed. Depending on the intensity of the stresses, the material within the specified domain is separated into low, intermediate, or high density finite elements [1]. The process is iterative, therefore, the structure with altered densities is analysed until convergence is reached and the result that is expected to be achieved is to have a clear separation of high and zero densities (voids). VDM is a discrete method that does not allow for intermediate densities, unlike SIMP which is continuous and thus includes intermediate density values [11,20,32,34,43,44]. VDM is identified as a cost-efficient approach. The VDM method and the SIMP interpolation scheme, are perhaps the most widely used and accepted approaches to topology optimisation of linear elastic and isotropic problems. Many adaptations and variations of the SIMP interpolation scheme have been used for a wide variety of applications outside of the linear elastic and/or isotropic remits of the original formulation [11]. Optistruct from the commercial software package HyperWorks [3] is a linear static solver using VDM and SIMP while the model has been set up using static loading only.

1.2. Topologies

Topologies often resemble complex natural forms; it is therefore often up to the designer to interpret them. Interpretation is a crucial part of the overall optimisation process and needs to be performed carefully with consideration of manufacturing and practicality factors. This has been majorly unaddressed in existing literature. 2D approaches, such as that taken by Anand and Misra [4], have proven to be effective for identifying a range of potential cross-sectional shapes with a wide variety of load and support conditions. The study was conducted using the FE software ANSYS and presented stress-plots with optimal topologies for column and beam cross-sections. Bochenek and Tajs-Zielińska [6] used a minimal compliance objective approach to optimise extruded columns with different support constraints (pinned and fixed) and subjected to a transverse distributed load representing buckling in one or two planes. Optimal topologies and their corresponding critical buckling loads were then obtained. Through the 3D approach, the study has also demonstrated variations in bending and shear along the length of a column result in a non-uniform cross-section. Zuberi et al. [45] attempted to overcome the variation issue through the use of an extrusion constraint in topology optimisation of beams, as explained later in this paper. However, it is evident that the resulting cross-sections are limited to overly simplistic shapes, which are likely susceptible to local buckling phenomena due to the slender thin webs. Tsavdaridis et al. [43] applied topology optimisation technique in the design of perforated I-section beams. The study implemented a minimal compliance approach in order to create a unique optimal web configuration. Thereafter, nonlinear FE buckling analyses were performed on short sections of the optimised and cellular beams for comparison. The optimised section was found to have a higher buckling stiffness, therefore validating the effectiveness of the application of design optimisation on structures.

1.3. Aluminium

In the field of civil engineering, aluminium, and its alloys have found increased structural applications as a result of their architectural appeal and special physical characteristics along with intensive relative scientific research and the development of codified provisions. Among others, materials' low density, allowing reduced loads on foundations and easier construction processes along with its excellent corrosion resistance leading to limited maintenance requirements as well as the extrusion feature which is facilitating the production of customised cross-sections that provide significant advantages in construction [28]. In particular, although available for some other non-ferrous metals, such as brass and bronze, it is with aluminium that the extrusion process has become a major manufacturing method [31].

The extrusion process allows aluminium sections to be formed in an almost unlimited range of cross-sectional shapes, resulting thus to more options for tailored solutions to structural problems, while a significant advantage is the ability to produce sections that are very thin relative to their overall size [13]. During this process, the hot metal is forced through a die with a specific cross-sectional shape profile as shown in Fig. 1. More recently, a new manufacturing process to create metallic sections using the modern technique of additive manufacturing has been introduced by engineers. As Tsavdaridis et al. [42] mentioned, when compared with 3D printing, extrusion can produce longer span members, at a faster rate with fewer imperfections. However, 3D printing creates a greater variety of cross-section shapes as it does not require the pre-production of a die. Additionally, extrusion is only able to create members with a constant cross-section shape along the member length whilst 3D printing can vary the cross-section shape along the length of the member. 3D printing is currently costlier than the extrusion process which also have a slight advantage due to its current widespread use. However, the costs associated with 3D printing are likely to reduce due to the reduction in the cost of components and raw material – fostering ultra-lightweight. With the adjacent reduction in cost and material usage, thus the impact on carbon footprint, the use of 3D printing is about to become more widespread. A drawback to 3D

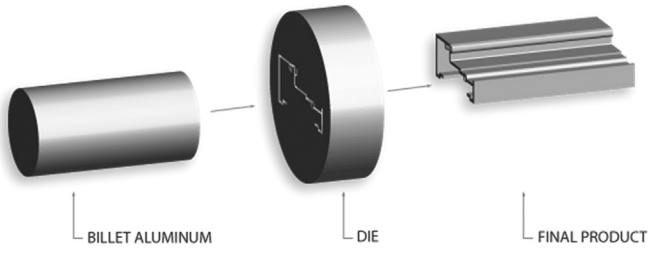

Fig. 1. Schematic of die extrusion process [33].

printed members to date is their unknown behaviour. Extensive tests to analyse the behaviour of extruded sections for 3D printed sections are yet to be conducted.

On the other hand, aluminium's applications are limited within the construction industry comparing with steel projects, due to its relatively low elastic modulus (70 GPa); around 3 times smaller than the 200 GPa elastic modulus of steel [15]. It is a critical flaw when considering structural design since it determines bending deformation of beams and is linearly related to flexural and local buckling of columns. In order to compensate for the low elastic modulus and achieve higher stiffness (*EI*) of cross-sections, the moment of inertia has to be increased. Thus, any aluminium elements must have a cross-sectional shape with the moment of inertia increased by a factor of 3 to be competitive with steel. To achieve this dramatic increase of the moment of inertia, it is impractical to increase all cross-section dimensions by a factor of 3, as this triples the weight of the aluminium section, thus negating the weight savings gained by using aluminium instead of steel.

Gitter [15] noted that increasing the section depth by a factor of 1.4 whilst keeping the width constant results in a moment of inertia roughly three times larger whilst keeping a 50% weight reduction. However, increasing depth by a factor of 1.4 does not significantly increase the width-to-thickness ratio (or slenderness ratio) of the member which is a dominant factor when buckling is concerned. Consequently, buckling will be most likely unaffected by this design approach. In addition, the method increases the cross-sectional area, thus, again does not fully maximise the weight savings to be gained by using aluminium. A method which uses the same cross-sectional area whilst increasing the moment of inertia by a factor of 3 will fully maximise the weight savings. Sections obtained through topology optimisation can achieve a high I-value with an optimal amount of material and material distribution, hence the need for such studies.

When compared to standardised steel I- and H-profiles (Fig. 2a), through appropriate design and extrusion exploitation, structurally equivalent aluminium sections can be produced, which are deeper and lighter (Fig. 2b), have increased torsional stiffness (Fig. 2c), and ready to accommodate integrated functions (Fig. 2d). They are often asymmetric, more complex, contain thin walls and are reinforced with ribs, bulbs, and lips. Local instability is, therefore, the governing factor when designing such sections. Moreover, local and global buckling are more severe as a result of using aluminium, due to its low Young's modulus and thin walls to achieve weight savings.

Within this framework, the aim of the herein presented work is to investigate topology optimisation techniques' implementation in aluminium alloy structures, towards the design of novel profiles for beams and columns. Structural topology optimisation is considered appropriate to achieve efficient structural forms based on the principle of material distribution within a design space, in order to satisfy the applied loading and support constraints. It is intended to obtain improved geometrical properties of cross-sections and structurally efficient shapes in terms of strength and resistance to buckling. The target is to achieve minimum compliance, while potential weight savings can render significant reductions in mass production and construction costs. Consequently, this paper compares the proposed novel aluminium profiles with standard ones possessing similar mass aiming to assess the feasibility and applicability of the sections obtained through topology optimisation.

2. Design optimisation of aluminium profiles

2.1. Methodology

Previous attempts have been made to optimise structural members along with their length or their cross-section, yet both approaches have never been conducted together and compared. 2D modelling approaches, such as that taken by Anand and Misra [4], are effective for identifying a wide variety of potential cross-sectional profiles. Such models identify the stress-paths taken within the structure with low computational cost, allowing a wide variety of loading and support conditions to be examined. A limitation was that these models neglected the effects of variation in bending and shear along the length of the member, and are therefore of limited value. By comparison, 3D approaches are able to capture the complete behaviour of the member. The effect is that 3D models produce topologies with constantly varying cross-sections, and are thus impossible to manufacture using extrusion and other conventional processes. The added computational cost and complexity of these models then limits the detail of the models.

Thus, the design methodology for this study has been to perform and compare both approaches, as an attempt to compromise between the limitations. 2D models are formed from scratch and are then compared to cross-sectional slices taken from the 3D models at key points along their length. In this way, each of the relevant degrees of freedom identified in Fig. 3 has been considered and the study has been able to examine and validate a much wider range of cross-sectional profiles. This proposed optimisation including the post-processing method is referred here as the Sectional Optimisation Method (SOM) and it involves the understanding of the potential loading scenarios on the cross-section, effective material distribution, multiple overlaid results, and engineering intuition through the morphogenesis process (i.e., creating the final architecture of the cross-section). The process is summarised by the flowchart presented in Fig. 4.

Buckling constraints could have also been implemented in the same study during the structural topology optimisation phase so that the requirement on the structural stability tends to distribute the available material over a larger area. In contrast, the maximisation of structural stiffness caused the material to distribute along the load transfer path. The latter approach was adopted here while local buckling was checked in the post-processing step during the finite element analysis (FEA) stage.

2.2. Analysis parameters

As it was aforementioned, the topology optimisation study has been performed using Optistruct which has facilitated each step of the optimisation process from creating and meshing the FE model, through to exporting the final results to a preferred CAD package. All models have been analysed through a single linear static load-step.

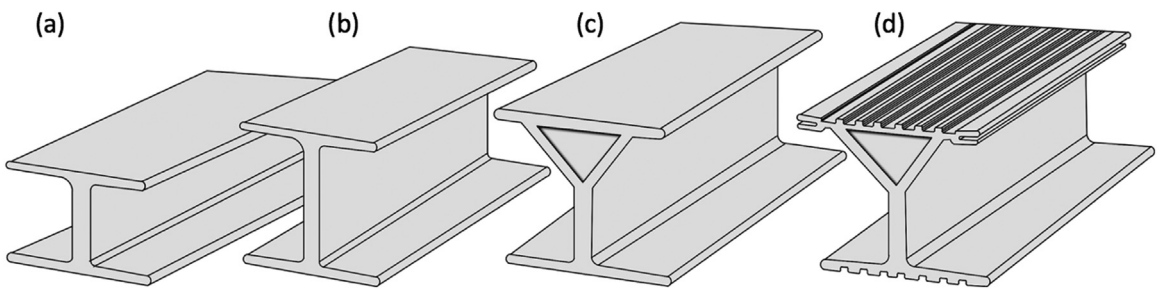

Fig. 2. I-section: Steel (a) and Aluminium varying forms (b–d).

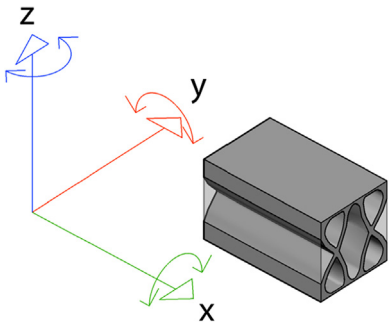

Fig. 3. Axes of translation and rotation.

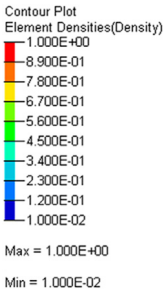

Fig. 5. "Key" of element densities.

2.2.1. Design variable

As Optistruct uses a built-in SIMP technique to solve topology optimisation problems, the design variable of the models has been the density of material contained within the finite elements. This density is able to take any value between 0 and 1, as demonstrated in the "key" shown in Fig. 5.

2.2.2. Objective function

The objective of the optimisation problem was to minimise the compliance of the structure, as it has been previously used in the literature [4,16,23,42,43,46]. The compliance is used to provide a measure of the strain energy within the structure, and may, therefore, be considered a reciprocal function for stiffness. Thus, minimising the compliance has the effect of maximising the stiffness, while less work is done by the load.

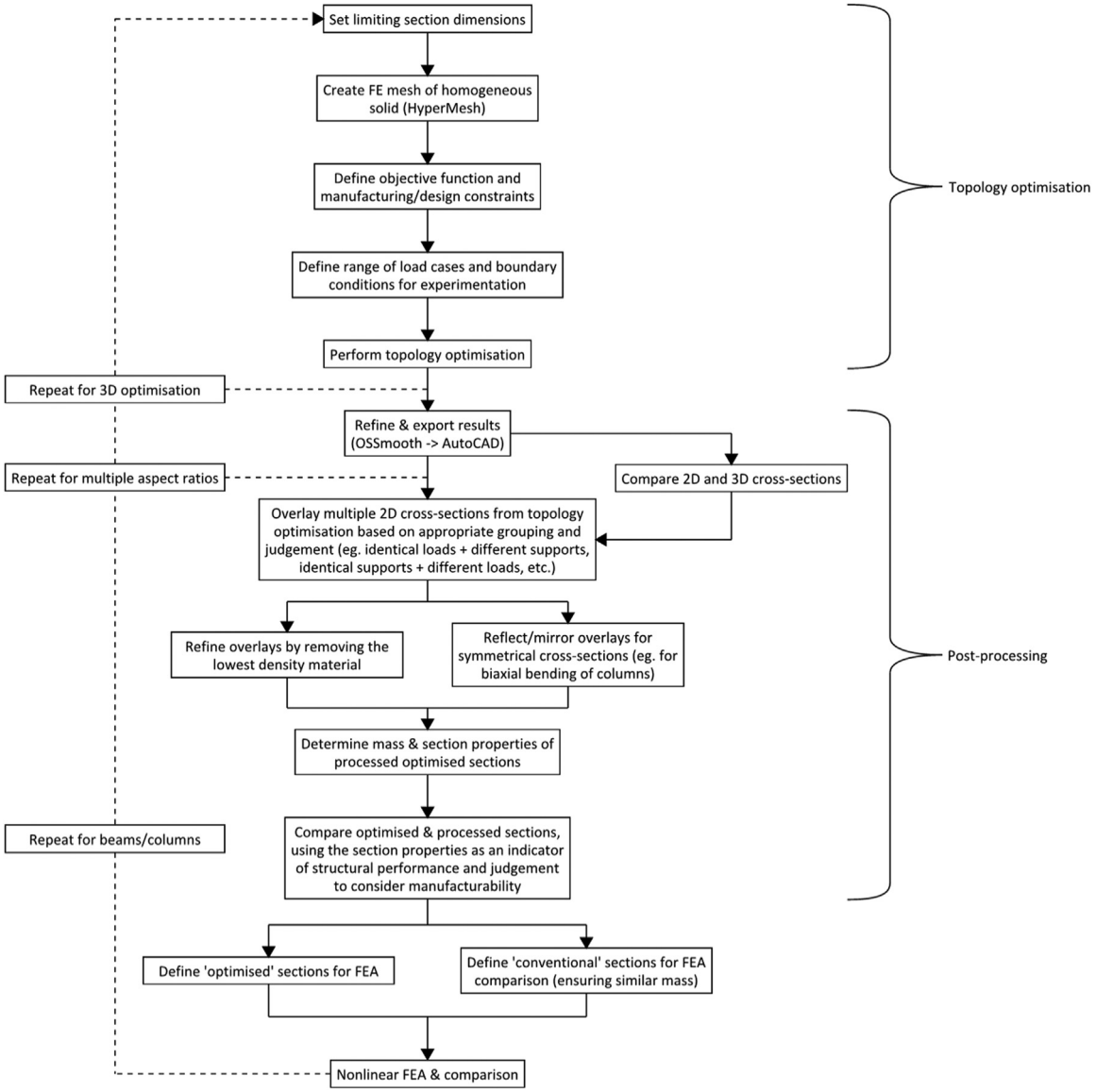

Fig. 4. Methodology flowchart.

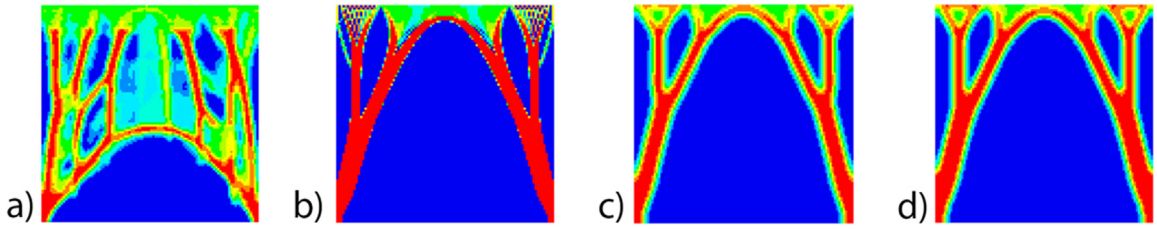

Fig. 6. Application of design constraints.

2.2.3. Design constraints

The primary design constraint on each of the models has been a limit on the fraction of the final volume in the structure to the volume of the starting design space. A range of values was experimented with, from 0.35 (35% of the initial volume) as in Fig. 6(a), and down to 0.25 as in Fig. 6(c). Following this, it was perceived that the value of 0.275 as shown in Fig. 6(d) provides the highest clarity of the result with an acceptable proportion of intermediate density elements.

2.2.4. Manufacturing constraints

Additional constraints have then been applied to the models to improve their clarity and ensure that the resulted configuration may be easily manufactured. These have been developed in a trial-and-error process as shown in Fig. 6, as this enabled the effects of each constraint value to be thoroughly explored. Fig. 6(a) first demonstrated the necessity for a single vertical plane of symmetry, to intensely improve the result to Fig. 6(b). A final constraint on the minimum member size was then added, to prevent the formation of the checker-board pattern of alternating 0 and 1 density elements seen in Fig. 6(b). A value of 7 mm was found to be the most suitable one and has been used throughout the remainder of the study. A methodology to the one described herein has been validated against previous optimisation studies for both the 2D and 3D cases [6,18].

2.3. Modelling parameters

2.3.1. Material properties

The optimisation has been performed on aluminium alloy 6063-T6, using elastic material properties as specified in Eurocode 9 [9]:

- Modulus of elasticity, E = 70,000 N/mm^2
- Shear modulus, G = 27,000 N/mm^2
- Poisson's ratio, $\nu = 0.3$
- Density, $\rho = 2700$ kg/m^3

It is important to note that the specific material properties do not affect the optimisation results, as is demonstrated by a direct comparison between the aluminium properties listed and those for S355 grade steel as provided in Eurocode 3 [8]. Fig. 7 depicts the results achieved while subject to an identical analysis, in which it is apparent that the results are the same and independent of the material at this stage. Specific alloy properties are, therefore, not listed until they take effect during the subsequent FE analysis stage when the performance of the members is tested (stress analysis).

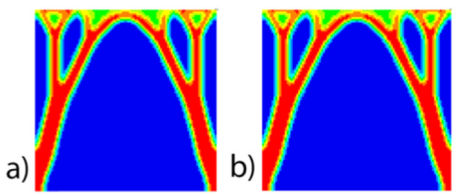

Fig. 7. Material Comparison: (a) Aluminium alloy 6063 and (b) S355 steel.

2.3.2. Geometry and mesh

As the scope of the study has been to optimise cross-sectional shapes for both beams and columns, the initial design space has been kept regular in order to provide maximum flexibility when processing and refining the results. Therefore, the majority of 2D and all 3D optimisation studies have been performed using a square design domain of 100 mm × 100 mm. However, additional aspect ratios of 2:1 and 1:2 have also been analysed for further understanding of the outcomes' applicability. As it is demonstrated in Fig. 8, these alternate aspect ratios achieve similar topology results. Hence, it has been concluded that the use of a square design domain is satisfactory, as any created cross-sections may be adapted into similar rectangular forms as required.

Shell elements with a nominal size of 1 mm have been used for meshing 2D models, enabling an efficient mesh to be achieved within the regular design space. These elements have a unit thickness to indicate the simple 2D form and include the six degrees of freedom previously identified in Fig. 3.

The 3D models for both beams and columns feature the same square cross-section with a member length of 2 m. As a consequence of the increased computational cost of the 3D models, it has been concluded to model these using 5 mm cubic solid elements following a mesh convergence study. As the cross-sections developed from the 3D cases are not used for detailed post-processing of the sections, the coarser mesh has been considered acceptable for the purpose of creating indicative slices along the length of the members.

2.3.3. Loading and support conditions

Forty different combinations of loading conditions, support conditions, and aspect ratios have been analysed, designed to produce members that are resistant to typical failure modes experienced in aluminium beams and columns such as buckling, local instabilities, and yielding under axial compression. Each of the load cases is shown in pair with the relevant contour plot of element densities and includes a depiction of the final cross-section for clear visualisation of the stress-path connecting the forces to the supports. It is important to note that as the optimisation uses a unit-less system, the specific magnitude of the load applied to the models is not of importance, but the geometry and relative distribution of the load affects the stress-paths within the cross-section. The selection of load distributions used for analysis has been chosen with reference to the guidance on cross-section classification according to Eurocode 9 [9].

2.4. Optimisation results

2.4.1. 2D results

The individual results presented in this section have been grouped into categories based on their loading and support conditions, so as to develop a narrative of how subtle changes to the input alter the behaviour of the stress-paths within the cross-section. The first set of results shown in Fig. 7 demonstrates a simple case of a cross-section subjected to a uniform load to the top flange and two pinned supports to the two bottom outer nodes. The three models are: (a), (b) and (c) - each has different aspect ratios in order to establish that the square cross-sections developed may be adapted into a similar rectangular form.

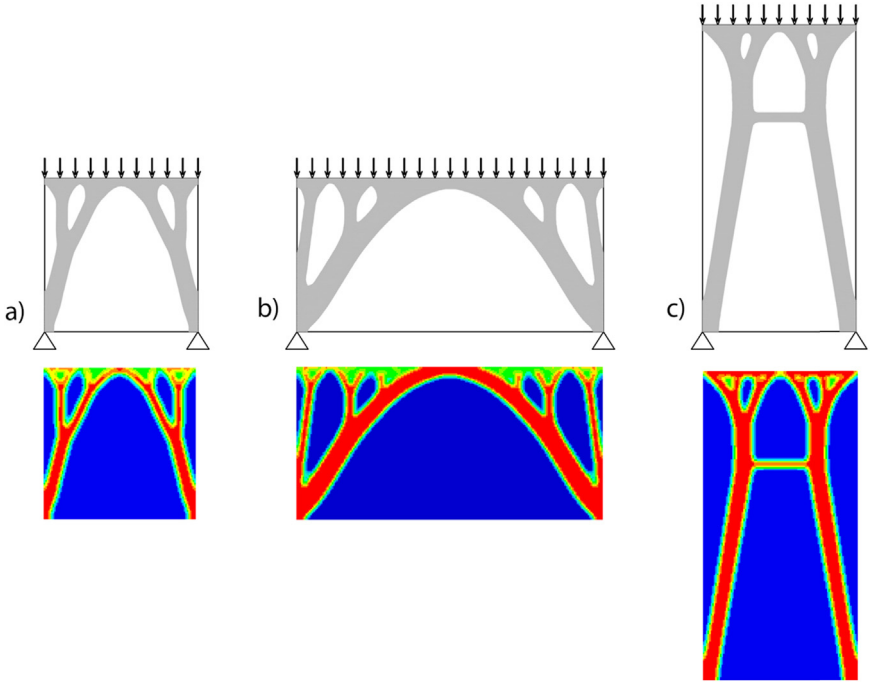

Fig. 8. Uniform compression with simple supports and varying aspect ratios.

The following sets of results show a variety of load cases including variations of shear, bending, torsion, and compression. Such stresses may be found in different locations (cross-sections) along the length of the structural beams and columns. In each group, either the load or support conditions remain constant in order to provide a direct comparison between the variable parameter.

The effect of the uniform load on a variety of support conditions is explored (Fig. 9), and it was observed that the topology remains identical when the bottom flange is either fully fixed or fixed only with two pinned supports as in Fig. 8. Thus, it has not been considered necessary to analyse load cases with a fully fixed flange, and pinned supports are used throughout Fig. 10, in which the distribution of the applied shear load is varied.

The effects of bending induced through applied tensile and compressive forces are also explored (Figs. 11 and 12), and a direct distinction between the results of identical load cases with both varying aspect ratios and varying support conditions was obtained.

The effect of additional horizontal loads intended to introduce resistance to overturning and torsion into the cross-sections was further investigated and shown in Figs. 13 and 14.

2.4.2. 3D results

Through the 3D optimisation approach, the optimal cross-section which varies along the length of the member was explored and was used to provide a series of slices through the beam-column element with which to compare and validate the sections generated through the 2D analysis.

2.4.2.1. Structural beams. The 3D design space has been modelled as a uniform homogenous solid, causing the lines of principal stresses to match those in a concrete beam. As the topology optimisation software uses stress-paths to determine the optimal layout of material within the structure, distinct regions of low stress may be observed at each quarter of the span. It is observed that these regions correspond with the overlapping of the lines of principal tensile and compressive stress, and therefore, serve to cancel each other. Whilst the use of web openings and perforations at mid-span has become common practice in thin-webbed metal beams [37–41], these observations suggest that further

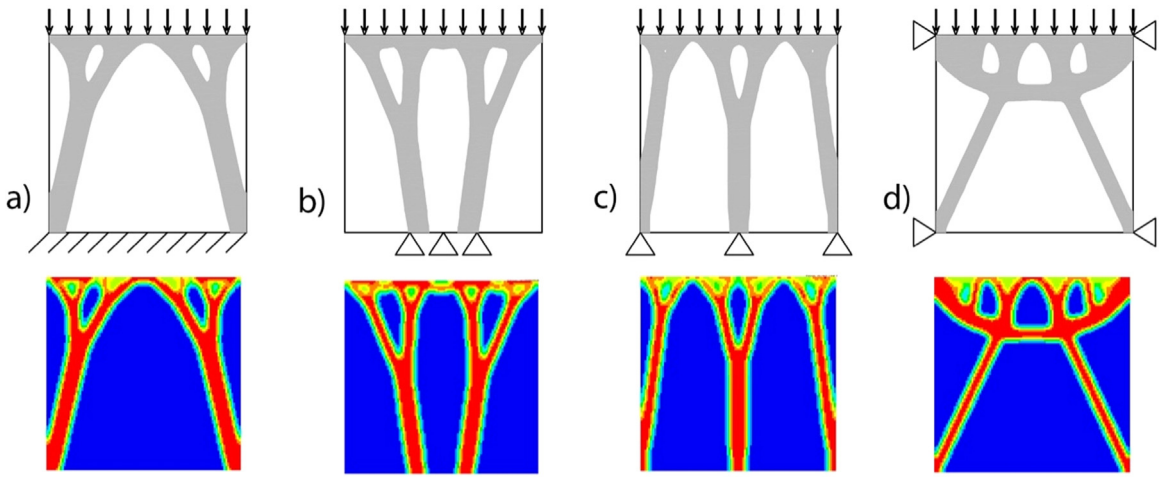

Fig. 9. Uniform compression with varying support conditions.

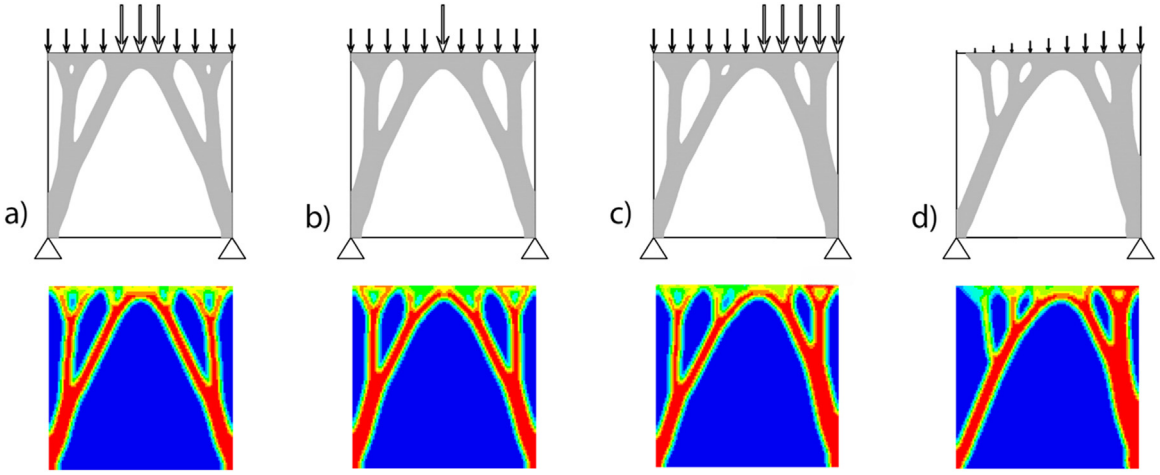

Fig. 10. Varying compressive and torsional loads to the top flange.

material savings could be made through the reduction of the section at additional points along the beam's length – thus could be used for sustainable design of lightweight beams made of other materials too.

A total of six different loading and support combinations have been analysed for the 3D models of beams to obtain an indicative overview of the optimum material distribution. Fig. 15 shows the effects of a uniform pressure to the top flange, whilst Fig. 16 demonstrates how the cross-sections vary when bending is applied through perpendicular forces to the top and bottom flange in order to produce a doubly-symmetric member.

2.4.2.2. Structural columns. 3D optimisation was performed on an extruded 100 mm × 100 mm square column of 2 m height with fixed-pinned supports as shown in Fig. 17(a). The box shape of the cross-section could be attributed to the fully symmetric profiles obtained through 2D optimisation. An axial compressive load was applied at the top and loads triggering buckling in two planes – in the middle of the member. Symmetry manufacturing constraint was applied to the model about y–y and z–z axes. When subjected to two-plane buckling the column developed concentrations of material at the four corners (Fig. 17(b)), resembling a box section at multiple locations along the length of the member. Formation of a web connecting the flanges is also observed in the middle of the member at the location of the lateral load.

2.5. Comparison of results from 2D and 3D models

As it was aforementioned, the 3D optimisation method reflects more accurately the behaviour of structural members but comes at an increased computational cost and post-processing operations. This is clearly demonstrated in the larger element size of the 3D mesh shown in Fig. 18(a and b), in comparison to the 2D meshes showing much greater clarity throughout Figs. 6–14. The increase in clarity strongly benefits the post-processing process of SOM discussed in the following section.

However, the cross-sectional slices produced by the 3D method play a significant role in validating the results of the cross-sections achieved from the 2D method such as that discussed within this paper, and numerical methods such as that adopted by Kim and Kim [22]. The similarity observed between the cross-sections shown in Fig. 18(a and c) and (b and d) demonstrates the rationale of using the smoother 2D results during the post-processing of the results.

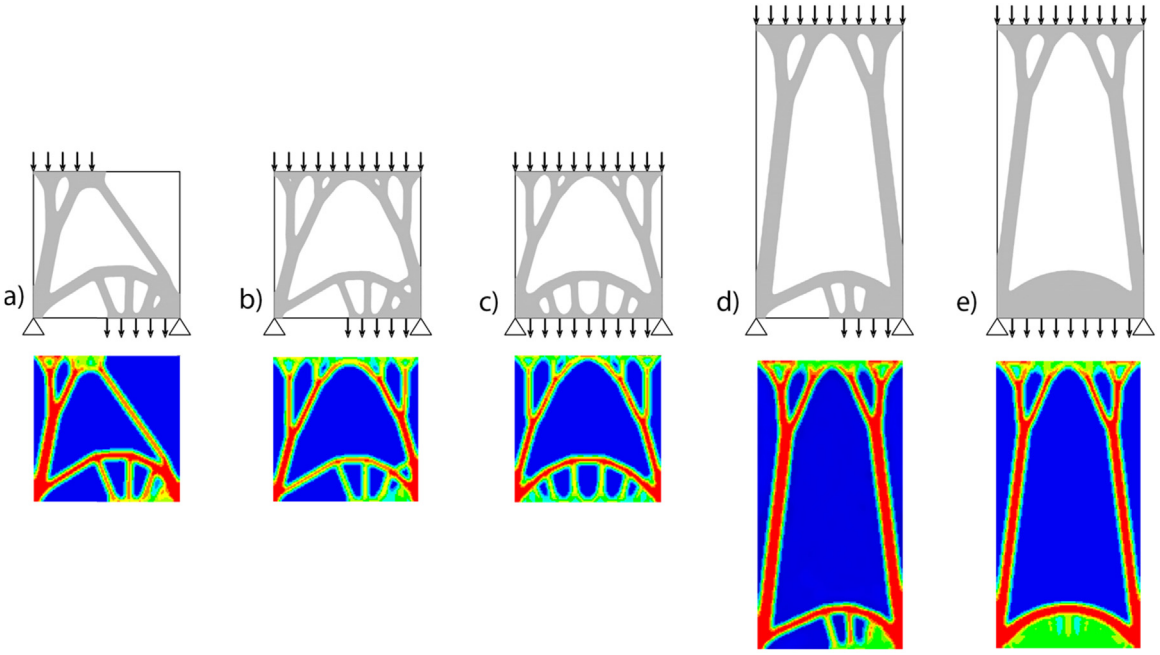

Fig. 11. Varying compressive and tensile loads with two supports.

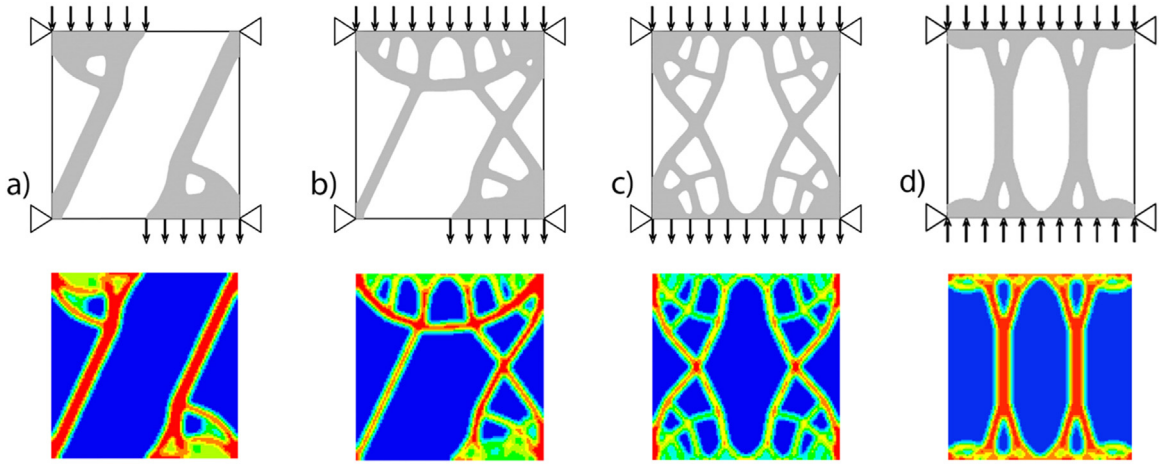

Fig. 12. Varying compressive and tensile loads with four supports.

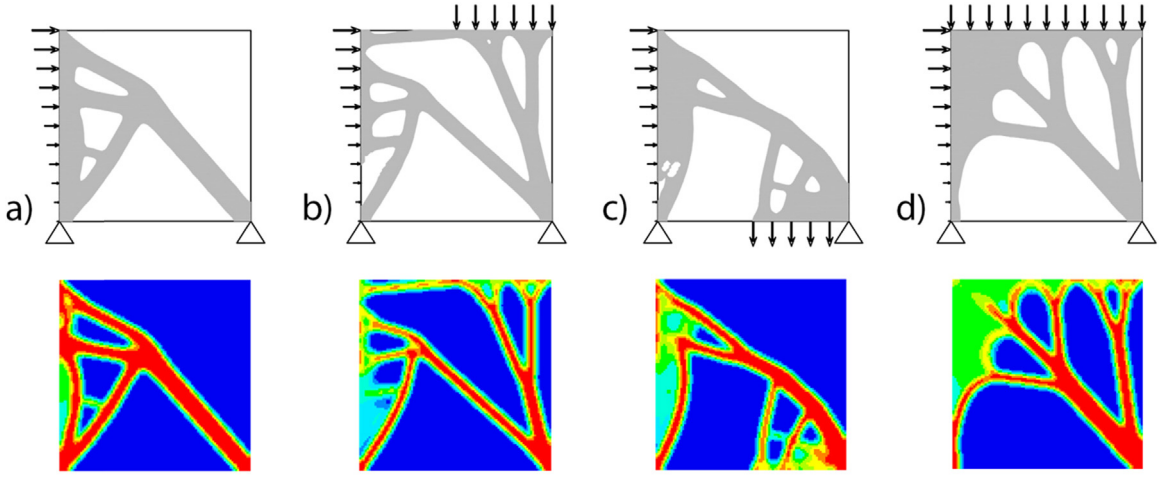

Fig. 13. Torsional loads through varying vertical and horizontal forces.

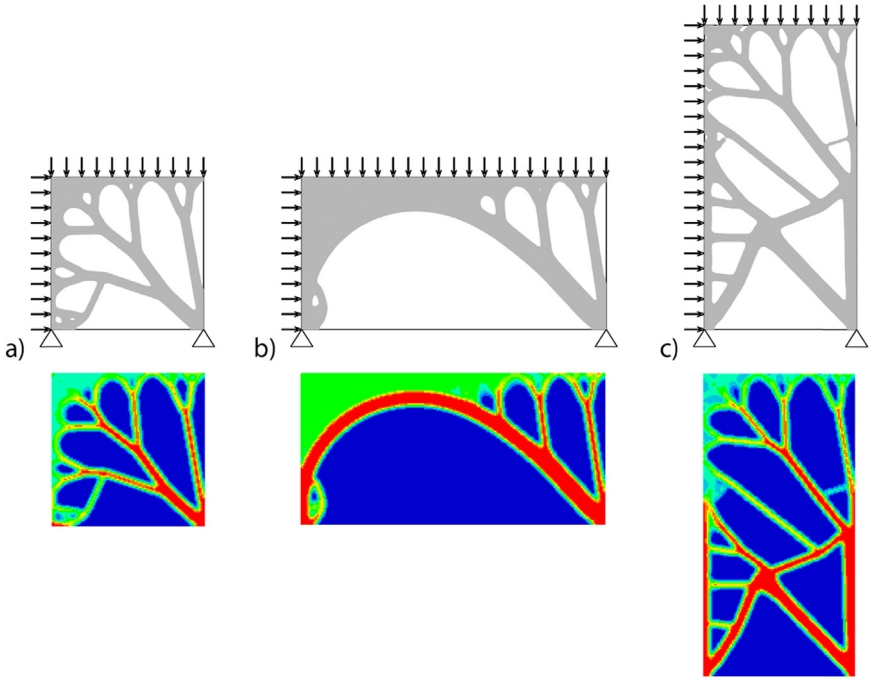

Fig. 14. Torsinal loads with varying aspect ratios.

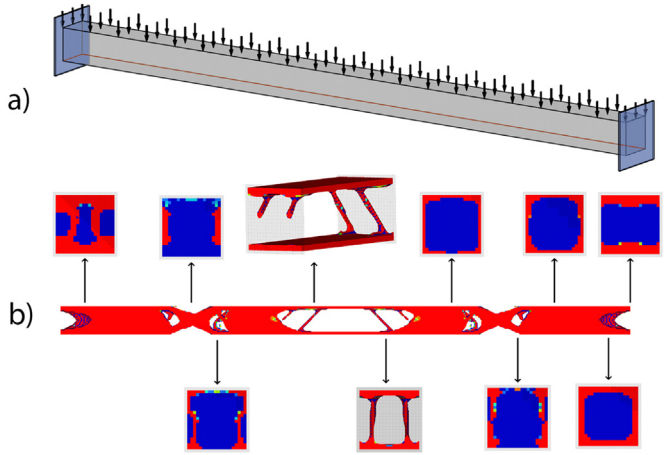

Fig. 15. Fixed beam with pressure to the top flange: (a) input and (b) results with cross-sectional slices.

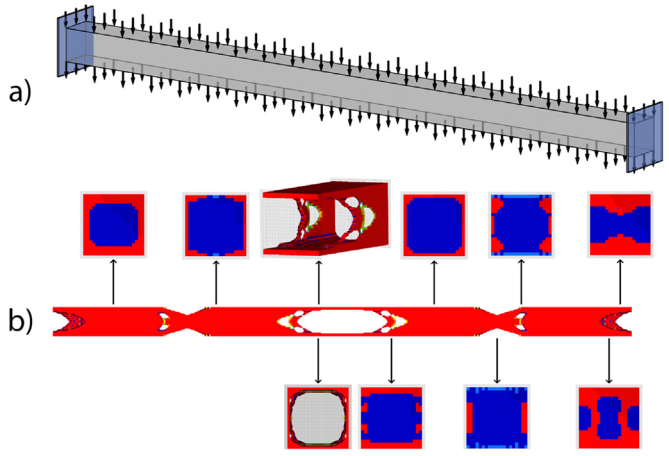

Fig. 16. Symmetric fixed beam: (a) input and (b) results with cross-sectional slices.

2.6. Post-processing

Following the topology optimisation results, careful interpretation is carried out for the development of realistic structural configurations for cross-sections while considering today's design practices' and manufacturing limitations. The results are sensitive to the geometry and so a method of post-processing multiple results to allow for these sensitivities is proposed in this paper. The 2D contour plot results shown previously have been smoothed with a default density threshold of 0.3 using Altair Engineering's OSSmooth (built in HyperMesh post-processing tool). The density threshold is related to the density slider in HyperView and specifies the mesh to be used for the post-processed geometry.

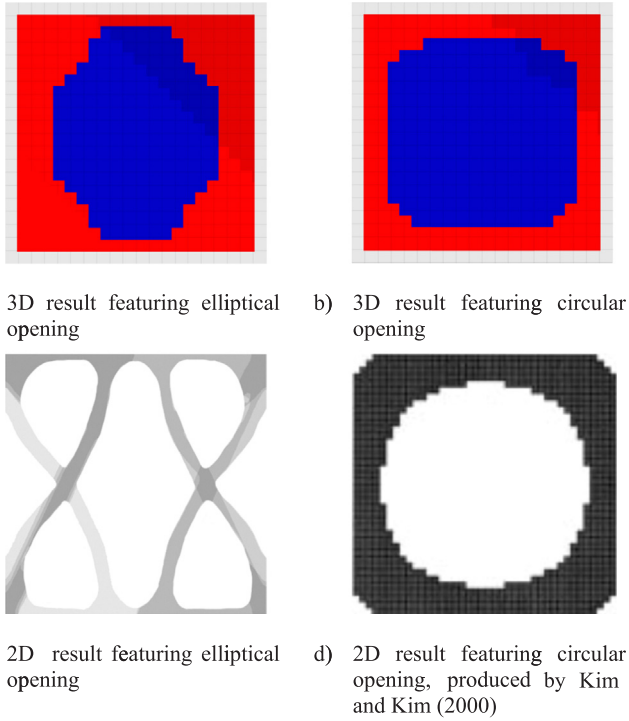

Fig. 18. Comparison of cross-sections resulting from 2D and 3D optimisation methods.

In order to produce cross-sections that would achieve the highest stiffness, a post-processing approach (part of SOM) was developed, which is completed in four steps:

1) For the sections to be resistant to multiple loading conditions, certain resulting topologies were overlaid and presented in a form appearing similar to X-rays (slices).
2) In some cases, the resulting shapes were mirrored about one or two axes to provide resistance in more than one direction as found in typical column sections in practice.
3) The most frequently stressed material patterns of the sections were identified - darker in colour.
4) Employing engineering intuition; the sections were manually processed and new shapes were carved based on the interaction of the overlaid material to allow for the interaction of various load cases to be considered.

2.6.1. Beams

2D optimisation results provide accurate model of stress-paths

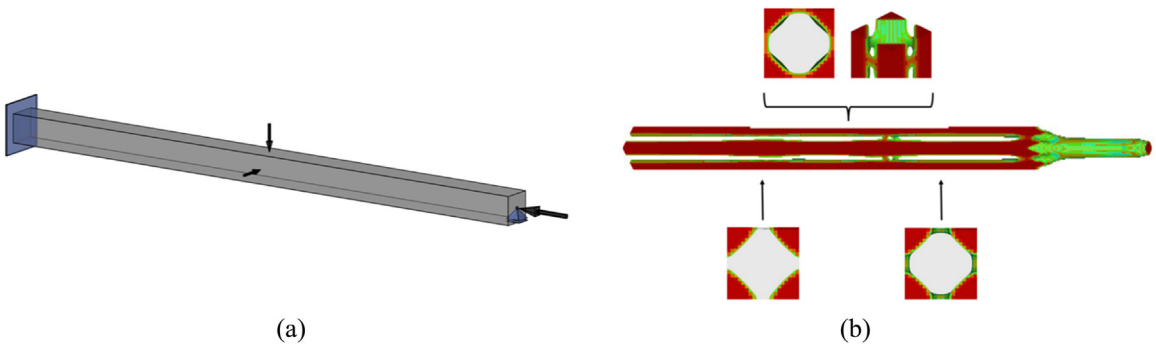

Fig. 17. (a) 3D optimisation input and (b) resulting topology with cross-sectional slices.

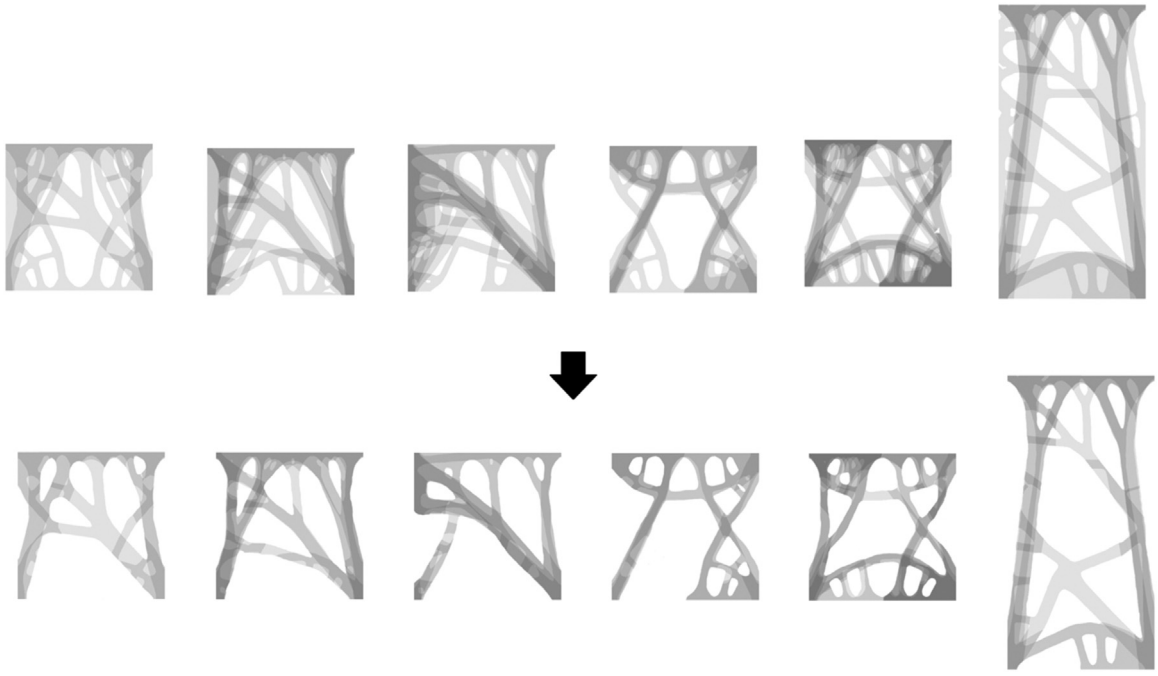

Fig. 19. Overlaid 'x-ray' results and simplification process.

under specific loading conditions, however, it is demonstrated that these load paths are highly dependent on the applied load. Consequently, SOM compares and combines a variety of these stress-paths to identify common parameters. To achieve this, individual topologies have been made transparent and overlaid, to enable shared material topology to appear darker, and hence easily identify the most commonly stressed material within the cross-section. This has been achieved by importing the 2D topologies produced into AutoCAD to allow the overlapping.

In order to propose a practical cross-section, the topology results have been grouped based upon the loading and support conditions. In this way, cases with the same loads but varying supports, and vice versa, are overlaid for a fairer comparison. Further combinations have then been included using engineering judgment to combine bending and torsion, as the primary loading considerations for a beam, as well as axial compression and bending for columns. Following this procedure, the final step was to simplify the final cross-sections by removing the lighter coloured (thus, rarely stressed) material as demonstrated in Fig. 19. This practice is employed to provide a final section that is characterised by its simplicity and the ease of manufacturability. As a result, the process can be subjective and in some cases, identical sets of results have been interpreted into different final cross-sections and vice-versa.

It is apparent that this method of post-processing could yield multiple cross-sectional profiles, thus certain selection criteria have been utilised in order to determine which sections to put forward for further FE analysis. It was deemed suitable that two optimised cross-sections should be analysed in order to provide an adequate representation of the suitability of SOM. Therefore, the structural properties of the five profiles which deemed most practical have been further analysed and compared. As the manufacturability and aesthetically-based criteria (such as the variation of plate thicknesses and number of voids) are difficult to quantify without precise manufacturer specifications, they have been omitted from the selection process and are only included within the refining process at a later stage when manually removing the material that is infrequently stressed.

Cross-sectional area, moment of inertia, and radius of gyration properties have been determined for each one of the five selected cross-sections and presented in Table 1 for the beam cross-sections shown in Fig. 20.

Table 1
Optimised beam cross-section properties.

Section	A	B	C	D	E
Area [cm^2]	44.39	30.32	39.43	48.84	37.82
Moment of inertia, y [cm^4]	340.26	337.32	399.50	528.69	436.66
Moment of inertia, z [cm^4]	448.14	312.46	423.15	479.10	426.65
Radius of gyration, y [cm]	2.769	3.335	3.183	3.290	3.398
Radius of gyration, z [cm]	3.177	3.210	3.276	3.132	3.359

It is well documented in the literature [15,21] that symmetric cross-sections are preferred for the ease of the extrusion process. The asymmetric beam cross-sections A and D are limited in their application due to being optimised for torsion in one direction only and are therefore eliminated from the selection process while the structural properties have been used to identify the best two profiles. Table 1 confirms that the profile C is stiffer about the z-axis and the material is not used wisely, therefore, less suitable for bending about the major axis as beams most often experience. Its radius of gyration about the y-axis is also lower than profiles B and E, thus the latter two profiles have been selected for comparison through FEA.

For further comparison, an additional optimised cross-section has been included from the 3D optimisation study. This section (as shown in Figs. 16 and 18) appeared frequently and is also illustrated in earlier research by Kim and Kim [22] while performing a 2D optimisation study. Moreover, due to its symmetrical geometric parameters which makes it suitable for the traditional extrusion manufacturing process, this section has also been selected for comparison through FEA.

2.6.2. Columns

Column cross-sections found in practice are most commonly symmetric and have high buckling resistance about two or more axes depending on specific applications, hence the logic followed in developing the final cross-sections is shown in Fig. 21.

Profile A represents an optimised column profile developed by applying pure compression. The shape clearly resembles a standard double webbed compound column cross-section, making it a viable choice.

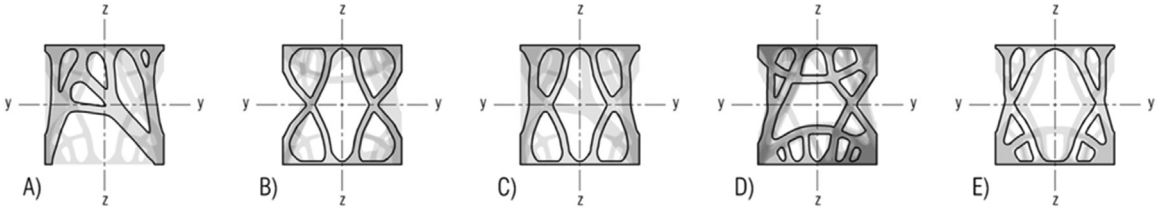

Fig. 20. Final SOM results of beam cross-section profiles.

Development of the other four cross-sectional profiles takes into account column behaviour under combined compression and bending, therefore, failure due to buckling. Sections B and C represent profiles of a column providing high stiffness in the y-axis. The profiles are a combination of resulting stress plots with loading replicating compression and bending of a member as it buckles. Therefore, they are applicable in cases where an eccentric axial load or a moment are applied triggering one plane buckling. Sections D and E are resistant to compression and buckling about the two axes, and they have equal stiffness in both axes while appear more resistant to local buckling due to the larger wall thickness. The section properties are presented in Table 2.

FFE models were then developed and analysed for the utmost optimised sections. The performance of these optimised sections was compared to standard beams and columns with similar mass. Performance criteria in terms of buckling load capacity and corresponding deflections were investigated. A comparative study was also established under the same project to validate the sections' feasibility and applicability. Results of this study are presented in Grekavicius et al. [16] and Tsavdaridis et al. [42] and demonstrated that the newly optimised sections outperformed some standard profiles.

Table 2
Optimised column cross-section properties.

Section	A	B	C	D	E
Area [cm^2]	35.36	49.95	52.00	59.13	49.10
Moment of inertia, y [cm^4]	461.63	565.23	582.67	608.38	442.67
Moment of inertia, z [cm^4]	224.58	449.33	578.80	608.38	442.67
Radius of gyration, y [cm]	3.61	3.36	3.35	3.21	3.00
Radius of gyration, z [cm]	2.52	3.00	3.34	3.21	3.00

3. Finite Element Analysis (FEA)

In this section, the scope was to select one of the most optimum profiles and to fully characterise its properties so as to be readily used in routine aluminium member design checks by engineers and ultimately proof the results of the above design optimisation studies. This paper only focuses on characterising the local buckling due to compression behaviour of the optimum profile. Making the section more appropriate for the traditional manufacturing process allows for both its mass production at low cost and thus the easy assimilation of novel sections. Consequently, design specifications and guidelines can be developed in line with other currently used metallic materials.

Commercial FEA software package Abaqus/CAE 2017 was used herein to assess the performance of the novel optimised cross-sectional shapes. A geometrical and material non-linear analysis was employed, which accounts for the plastic behaviour of aluminium performing a stub column test.

3.1. FEA parameters

3.1.1. Material properties

The same materials as before were chosen to remain consistent with the optimisation analyses, and so the properties of aluminium alloy 6063-T6 were adopted. The Ramberg–Osgood expression is typically used to describe the nonlinear stress and strain behaviour of such alloys [17]. Unlike structural steel, aluminium alloy 6063-T6 does not have a clearly defined yield point. Instead, the 0.2% proof stress is used to define an equivalent yield point before significant plastic hardening takes place [24].

Due to large variations in the types and properties of aluminium alloys, Eurocode 9 [9] Annex E suggests the best way to calibrate the properties of any aluminium alloy through a tensile test. This method was not used in this paper, instead, the nominal values found in Eurocode 9 [9] were employed. Linear modelling of material plastic behaviour was adopted. Annex E of Eurocode 9 [9] allows for modelling of aluminium plastic behaviour using linear models and for a bi-linear relationship (Fig. 22).

Residual stresses are usually insignificant for extruded sections [27] and their use in FE modelling has been shown to have little influence [25], thus residual stresses were not included in this study. Nominal values for the Yield Stress (f_p) and Ultimate Stress (f_{max}) of the 6063-T6 aluminium alloy are given in Eurocode 9 [9] and summarised in Table 3. The corresponding strain values of Plastic Yield Strain (ε_p) and Ultimate Strain (ε_{max}) were calculated.

An eigenvalue buckling analysis was performed while the most critical failure mode was the first eigenmode as this mode required the lowest magnitude of force to cause it. This agrees with Tsavdaridis and D'Mello [38] who stated that the first eigenmode with a specific scale of imperfection best reflects real-life behaviour. For extruded profiles, national specifications allow for a thickness deviation of 5% but this increases to 10% when thicknesses are less than 5 mm. This gives 0.5 mm as the worst-case value, therefore, 0.5 mm is the magnitude of geometrical imperfection used.

3.1.2. Boundary conditions and loading

Stub column tests can either be done with a fixed ended or pin-ended column (Fig. 23). The fixed ended arrangement is considered best for investigating cross-sectional instabilities or local buckling.

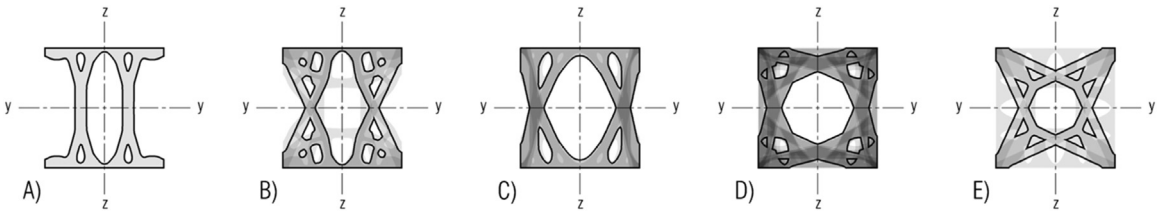

Fig. 21. Final SOM results of column cross-section profiles.

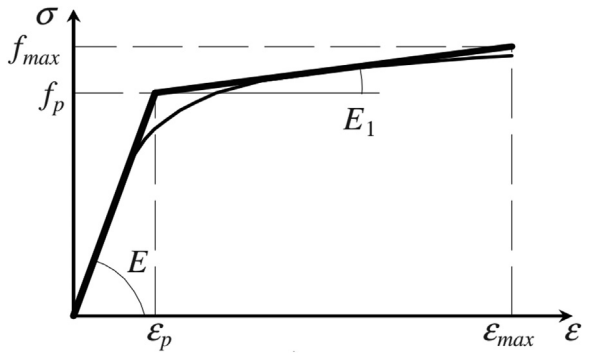

Fig. 22. Bi-linear stress–strain behaviour proposed in Eurocode 9 [9].

Table 3
Summary of material properties.

Material property	Value
Elastic Modulus	70 GPa
Density	2700 kg/m^3
Poisson's ratio	0.3
Plastic Yield Stress (f_p)	160 MPa
Plastic Yield Strain (ε_p)	0.0043
Ultimate Stress (f_{max})	195 MPa
Ultimate Strain (ε_{max})	0.106

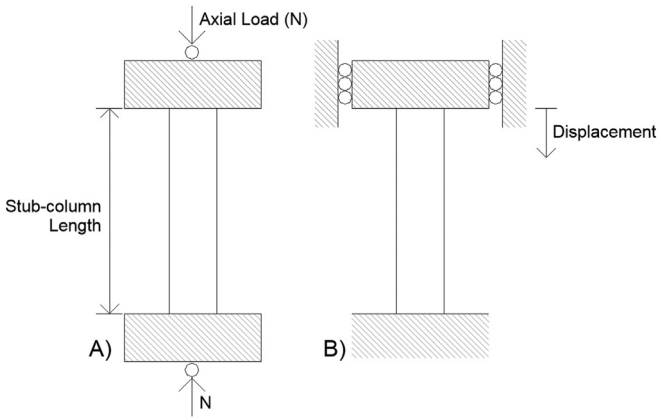

Fig. 23. Stub-column test setup. A) Pinned-end B) Fixed-end. Modified [29].

Mennink [29] noted that this is because in pin-ended columns, the centre of gravity of section shifts during the test resulting in an eccentricity in the applied load leading to an induction bending moment within the section.

To mimic a fixed end stub column test, rigid plates were used. These rigid plates simulated the interaction between the test machine and the column ends and were used to apply the axial load. One of the rigid plates is fixed and the other is only free to move axially towards the column, thus applying the compressive force required (Fig. 24). The column ends are constrained by the boundary conditions applied to the Reference Point (RP) at the centroid of the section. To model the fixed rigid plate, the 'encastre' condition was used with all degrees of freedom constrained. To model the movable rigid plate, all lateral displacements except the z-axis displacement were constrained.

3.1.3. Mesh convergence study and FE model validation

The irregular shape of this novel cross-sectional profile makes the use of a regular mapped mesh impractical and erroneous. Instead, a free mesh using triangular elements was able to achieve accurate results. The element type used is a 10-node tetrahedral element for the stub column as it can more accurately mode and capture any complex

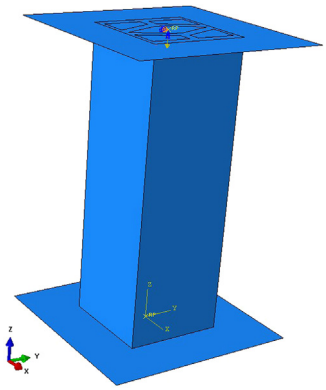

Fig. 24. Stub column test setup in ABAQUS.

interactions within the cross-section of the stuctural member being tested. The mesh sensitivity analysis and model validation were done simultaneously by comparing results from FE models with varying mesh sizes to experimental results from the literature.

The experimental model used for the mesh convergence and validation studies was the H70 × 55 × 4.2C-R section as used by Su et al. [35]. The FE model and experimental test outputs were compared using the following criteria: maximum load obtained, load-axial displacement curve, and failure deformation shape. The maximum loads obtained from the FE analysis (P_{FEA}) are very similar to the experimental result (P_{Test} = 196.9 kN) from Su et al. [35] as shown in Table 4. In addition, the failure deformation shape is similar to that obtained in Su et al. [35] as shown in Fig. 25. At last, the load-deflection data shown in Fig. 26 depicts that mesh convergence was reached when the mesh size reaches 5 mm. It is worth to note that there was a significant increase in the computational time due to the reduction in mesh size, thus a 5 mm mesh size was adopted.

4. Manufacturing criteria and morphogenesis process

Improving the cross-sectional profile and meeting the manufacturing criteria was paramount for the extrusion process, thus allowing for the ease of production of the optimised section. Extrusion can be more efficient when a uniform profile is used instead of the organic profile previously developed by the optimisation studies. Also, other rules used to improve the manufacturability such as to keep the maximum thickness ratio across the sections to 2:1 to fit within current extrusion limits, and that the new section should have a similar cross-section area and should perform similarly to the original optimised beam section.

Different sections were developed during the morphogenesis process refining the optimised results previously presented. Each alternative proposal design was developed as a modification of the original optimised profile for beams (Section B in Fig. 20). This shape can be identified as a square hollow section with five separate voids (i.e., one large central void surrounded by four other smaller voids). The parameters that mainly varied were the size and shape of the voids. Section performance was measured using the second moment of area, the radius of gyration, and the theoretical section compressive buckling load.

Table 4
Mesh sensitivity analysis results.

Mesh size	Element numbers	Node numbers	CPU time	P_{FEA} (kN)	P_{Test}/P_{FEA}
4 mm	38,121	62,275	44 min	186.9	1.05
5 mm	19,222	32,672	20 min	186.4	1.06
6 mm	12,036	20,806	7 min	184.1	1.07
8 mm	7906	13,448	3 min	180.5	1.09

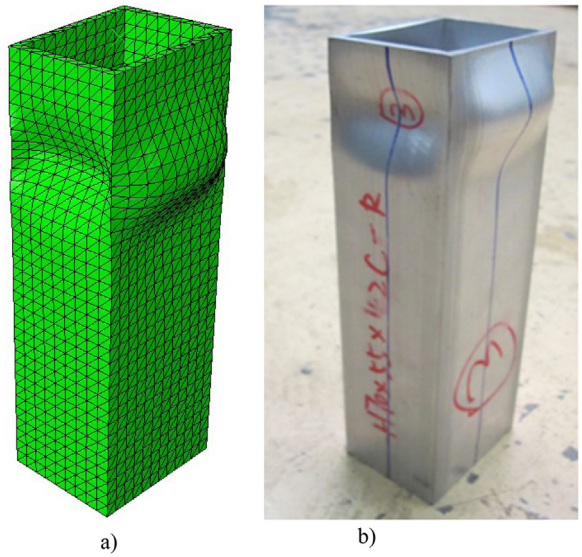

Fig. 25. Failure deformation shapes a) FE model and b) experiment [35].

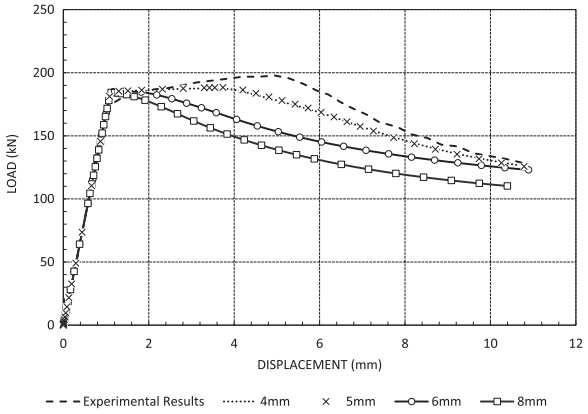

Fig. 26. FE mesh convergence and experimental results.

A variety of morphologies were developed based on the use of straight and curved elements; it was found that straight elements are ideal with respect to the second moment of area and radius of gyration. Consequently, this paper presents the results from the use of only straight elements. Variations in the potential sections come from the use of vertical or angled web elements. Under these restrictions, four potential forms or options were developed.

The first morphology (Option 1) closely mimics the previously developed optimised beam cross-section. The section is based on the idea that the original shape can be simplified as two flanges stiffened using two 'X' elements; the evolution of the profile design throughout morphogenesis is depicted in Fig. 27. Final designs of Options 2, 3, and 4 shown in Fig. 28(B–D) respectively, use vertical outer web elements to create shapes which can be effectively described as 'stiffened' square hollow sections. The variation between the sections comes from changing the angle of the internal web element. Options 2, 3, and 4 use internal angles of 44°, 22°, and 11°, respectively. Table 5 summarises the comparison between the initial optimised section and the new options.

4.1. Comparison of design options

According to Table 5, all new cross-sections have higher sectional properties than the original shape with respect to the second moment of area and radius of gyration. This demonstrates that the heuristic shape optimisation used was successful in terms of meeting both the performance and manufacturing criteria.

The following analysis is done using information from Table 2. Any references to the major and minor axes are the y–y and z–z axes, respectively. Option 1 provides the highest moment of inertia and the highest radius of gyration in the major axis. However, Option 1 has the lowest moment of inertia and lowest radius of gyration in the weak axis. Consequently, the section shape mainly uses its area to effectively provide stiffness in the major axis but due to the ineffective area use in the minor axis, the section may be susceptible to global buckling in the weak axis. Additionally, Option 1 has the lowest compressive buckling load due to slendered internal web elements, thus more susceptible to buckling.

Option 2 performs alike Option 1 in the major axis, but it provides a higher moment of inertia and radius of gyration in the minor axis. Hence, Option 2 utilises its area more effectively to provide cross-sectional stiffness in both the major and minor axis. Option 3 provides a higher moment of inertia and radius of gyration in both the major and minor axes than Option 4. Option 3 also provides a higher local buckling load. Option 3 is thus preferred to Option 4 due to the higher radius of gyration in both the major and minor axes.

Option 3 provides nearly double the buckling capacity of Option 2 while Option 3 provides a smaller radius of gyration in both the weak and major axes than Option 2. Option 3 is thus preferred to Option 2 due to the significantly higher buckling capacity. Option 3 provides a smaller major axis radius of gyration than Option 1, but it provides a higher buckling load than Option 1 and a higher radius of gyration in the weak axis. Consequently, Option 3 will be chosen as the best of the manufacturable sections developed in this investigation.

In view of cost-related aspects, production costs depend strongly on the rate of production and it is difficult to determine the accurate cost of a custom profile without having produced it [30]. However, regarding the developed profiles, a reliable preliminary cost estimation would have to consider the 6063-T6 aluminium alloy profile weight equal to 9–10 kg/m and the cost of the extrusion die at 3.000–4.000€, according to current data from industry.

5. Characterisation of cross-section in compression

The design of the members comes under the broad element behaviours of compression, tension, shear, flexure (bending) and torsion while Eurocode 9 – EC9 [9] provides guidance as to how these checks can be treated for standardised aluminium cross-sections. To investigate whether EC9 approach can be applied for the design of the optimised aluminium sections, extensive testing of the optimised sections is required. This paper deals with the behaviour under compression as the first critical test towards validation of these optimised aluminium profiles.

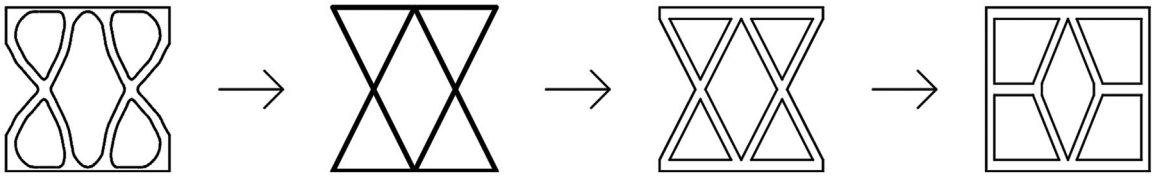

Fig. 27. Evolution of morphogenesis process to develop manufacturable designs (Option 1).

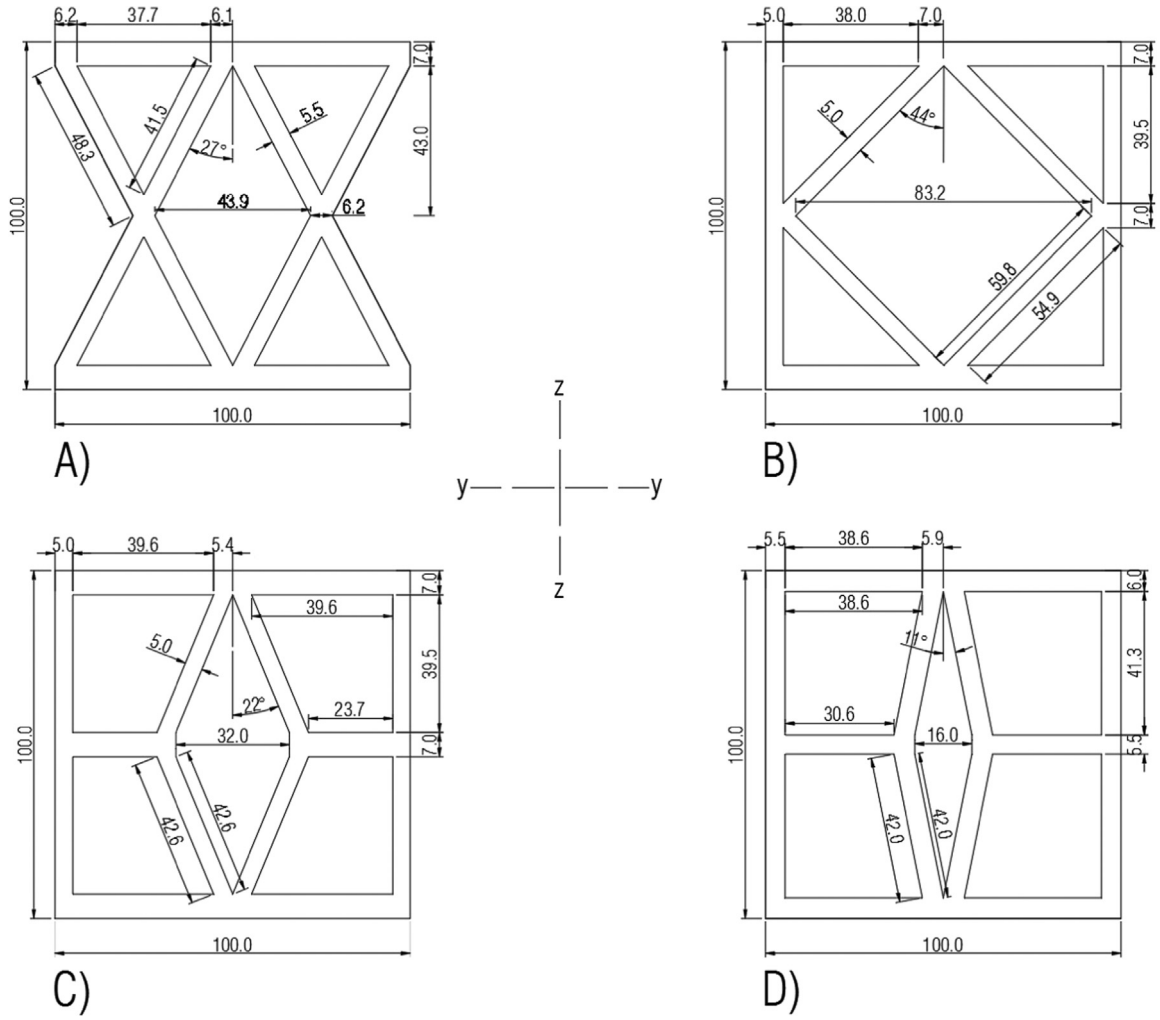

Fig. 28. 4No. Cross-sections to be considered under Option 1.

Table 5
Cross-section properties of new options compared to original optimised section.

Property	Original	Option 1	Option 2	Option 3	Option 4
Area [cm^2]	35.0	34.4	34.1	35.0	35.3
Moment of inertia, y [cm^4]	380	434	429	413	395
Moment of inertia, z [cm^4]	319	298	392	363	354
Radius of gyration, y [cm]	3.29	3.55	3.55	3.43	3.34
Radius of gyration, z [cm]	3.02	2.79	3.39	3.21	3.16
Local buckling load [kN]	1350	1289	785	1310	1078

5.1. Cross-section classification in EC9

Cross-section classification aims to predict how the proposed section is likely to fail. The section may reach its full potential, or local failures (local buckling) may cause the section to fail at an earlier stage. EC9 treats classification of aluminium members in a similar way to that of steel members, predominately based on the work of Mazzolani [26] as well as more recent improvements. EC9 places sections into four behavioural classes while these classes describe the global behaviour of sections under compression, flexure, or shear. Alike Eurocode 3 (EC3) for steel, in EC9 cross-section classes are defined by the capability of the section to reach the four defined limit states (Fig. 29).

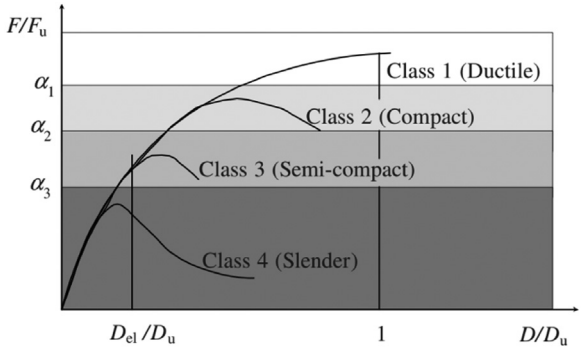

Fig. 29. Cross-section classes with respect to general section resistance [9].

5.2. Classification methods

The cross-section classification depends on the material proof strength, slenderness of the individual compression parts (i.e., width to thickness ratios of webs and flanges), the use of welds and the loading arrangement [19]. The cross-section components are split into three categories; flat outstand parts, flat internal parts, and curved internal parts. The width to thickness ratios of each cross-section component is then compared with the slenderness limit for each part. This approach, although simple and easily understood, only accounts for the buckling of each component individually, thus ignoring the additional

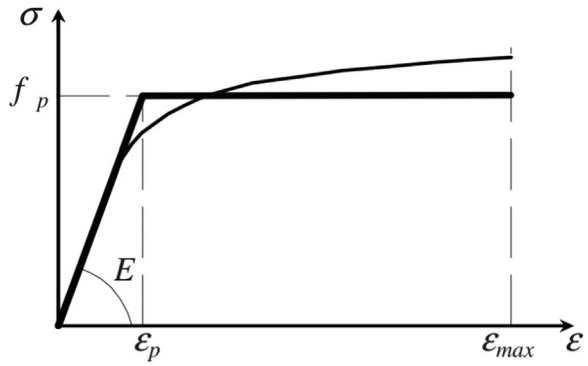

Fig. 30. Elastic-perfectly plastic model used in Eurocode 9 [9].

interaction between the individual components [29].

These additional interactions are more likely to occur in complex cross-sections, thus the simplified method and the slenderness limits proposed in EC9 may not be suitable for novel optimised sections. Additionally, cross-section classification in EC9 assumes a bi-linear elastic-perfectly plastic stress–strain model (Fig. 30) which ignores the advantageous behaviour of aluminium strain hardening [36]. For these reasons, Continuous Strength Method (CSM) is a relatively new cross-section classification method that has been developed to predict section behaviour. CSM accounts for strain hardening and the complex interactions between cross-section elements [36].

5.3. Parametric study

This section outlines the details and results from the parametric study to aid with the cross-section classification. During the stub column test, the overall buckling mode of the member must be eliminated to ensure failure is only due to local buckling [12]. To prevent overall buckling, BSI [7] recommends the stub column length should be less than 20 times the least cross-section radius of gyration (r). However, to exclude end effects noted that the minimum stub column length must be at least three times as long as the greatest cross-section width (B), thus the member length used was 3B [14]. All members used have a width of 100 mm, thus a member length of 300 mm.

The section flange and web thicknesses were varied to find out the effectiveness of existing cross-section classification techniques on the optimised cross-sectional shapes. The definitions of the flange and web elements are shown in Fig. 31 and Table 6 outline the dimensions of

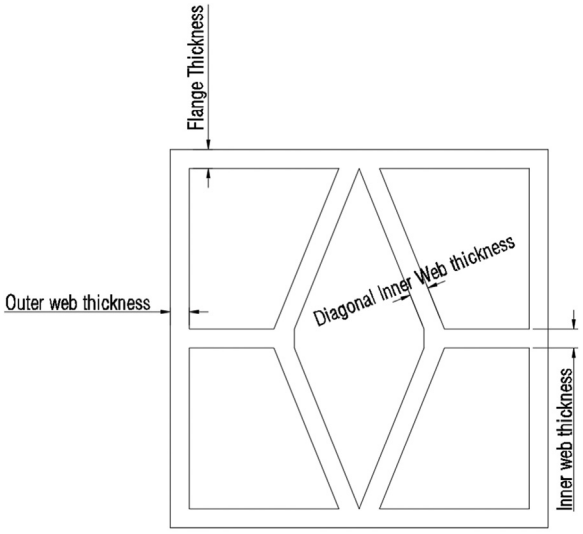

Fig. 31. Dimension definitions of section to be investigated.

Table 6
List of sections and geometrical properties.

Section number	Flange thickness (mm)	Web thickness (mm)	Cross-sectional area (mm^2)
1	5	5	3096
2	5	7.5	4074
3	5	10	5005
4	7.5	5	3502
5	7.5	7.5	4433
6	7.5	10	5317
7	10	5	3908
8	10	7.5	4792
9	10	10	1098

Table 7
Comparison of section classification between FEM and EC9 results.

Section number	Initial EC9 class	FEM class
1	Class 1	Class 3
2	Class 1	Class 1
3	Class 1	Class 1
4	Class 1	Class 1
5	Class 1	Class 1
6	Class 1	Class 1
7	Class 1	Class 1
8	Class 1	Class 1
9	Class 1	Class 1

flange and web thicknesses.

Each section used in the FE study was then classified according to the rules found in EC9 and the results are summarised in Table 7.

5.3.1. Results

The FE results are presented in Fig. 32 as a stress–strain graph. Figs. 33–36 depict the typical local buckling failure modes exhibited. Table 7 compares the section classification in EC9 to the class behaviour shown from the FE analyses. The 'FEM class' column was derived from interpreting information from the stress–strain graphs in Fig. 32. All the sections are 'Class 1' according to EC9. Of the sections tested, 9 out of 10 have the same 'FEM class' as that from EC9. The only section with a 'FEM class' different to that of EC9 is Section 1 which has the lowest both web and flange thickness tested in this study (see Table 6) – that was considered as Class 3. No Class 2 sections were considered as in all other cases (apart of Section 1) the cross-sectional stress stays above the ultimate stress value until failure.

6. Discussion and concluding remarks

This paper presents a structural topology optimisation study and proposes an incremental optimisation-based design approach, referred as Sectional Optimisation Method (SOM), combining advanced optimisation algorithms, multiple 'X-rays', heuristic optimisation and engineering intuition (morphogenesis process) on 2D and 3D models with a focus on the manufacturability and cross-section classification for aluminium cross-sectional design.

The optimised cross-sections are subjected to a variety of load-cases and the resulting patterns (mass distribution) were used to create new aluminium profiles. A series of unique topologies for a square 100 mm × 100 mm cross-section are generated using the SIMP technique found in Optistruct. SOM is employed for post-processing the 2D results aiming to address stability and manufacturability criteria. Different density plots are overlaid to identify the most frequently stressed areas of the cross-section, resulting in five novel section profiles for beams and columns. A 3D optimisation approach is then employed to identify the correlation between 2D and 3D results.

Both approaches for beams and columns predominantly result in

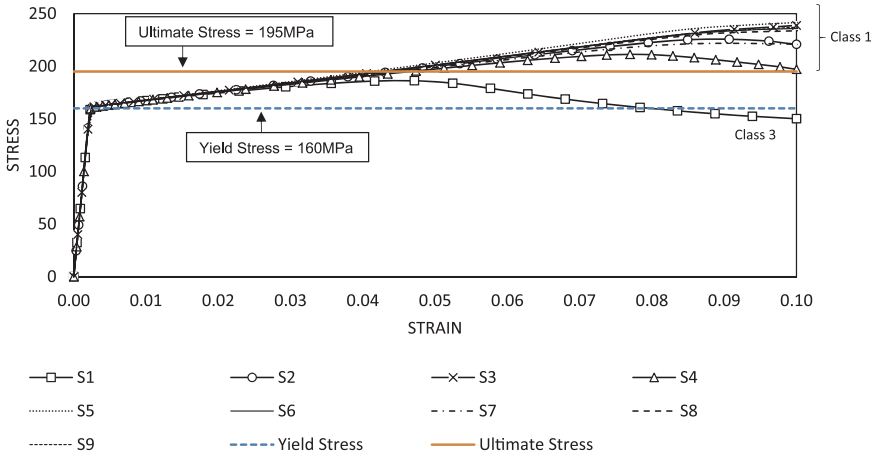

Fig. 32. Stress–strain curves for cross-sections tested in FEA.

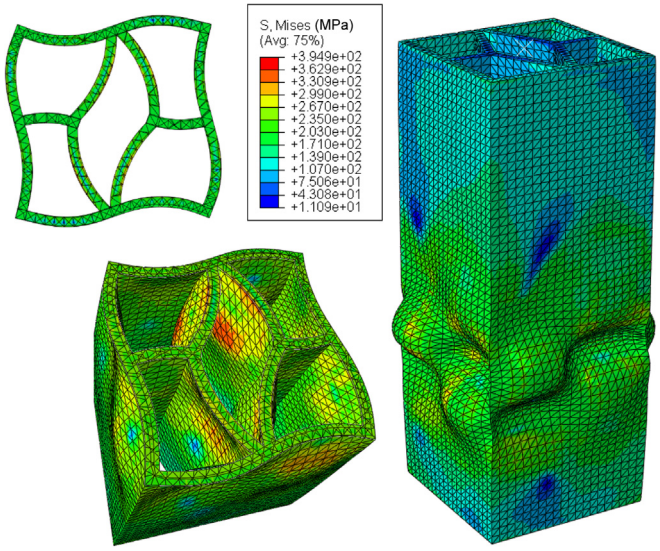

Fig. 33. Section 1 stub-column failure mode in FEA.

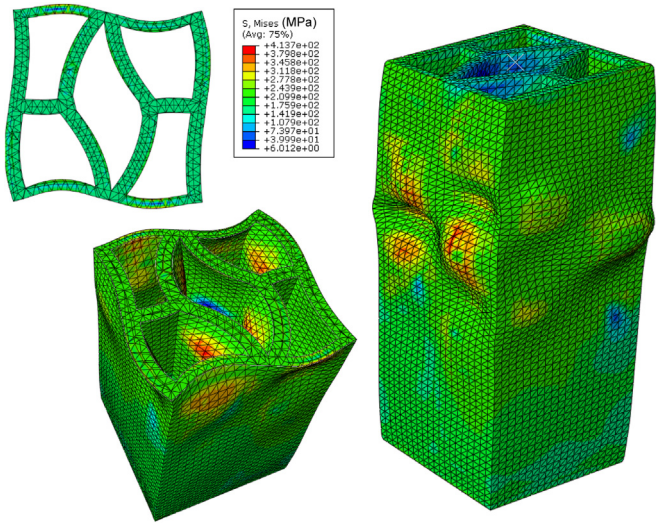

Fig. 34. Section 2 stub-column failure mode in FEA.

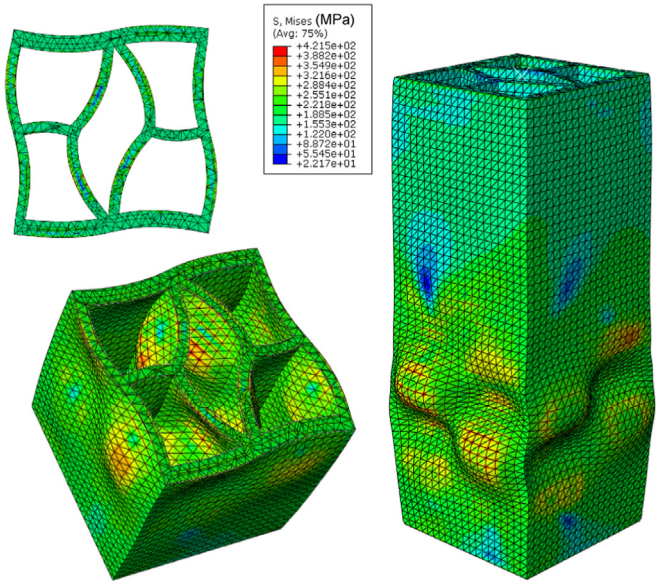

Fig. 35. Section 4 stub-column failure mode in FEA.

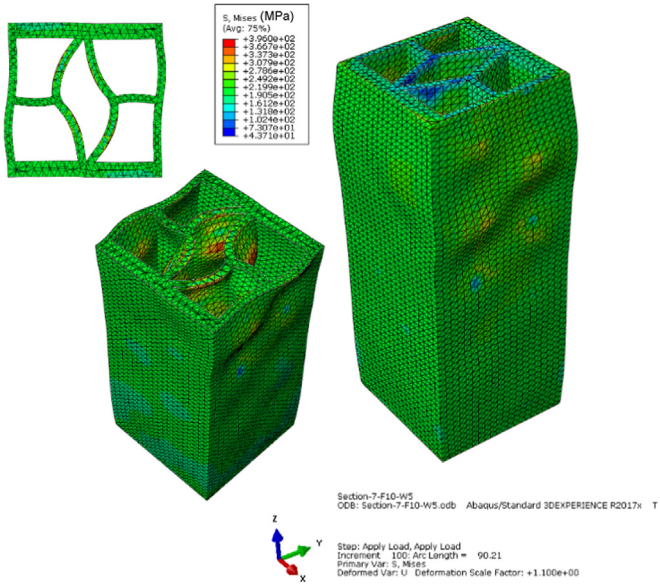

Fig. 36. Section 7 stub-column failure mode in FEA.

rather irregular hollow-based sections, including square-based profiles with a large central circular- or elliptical-type hollow in the middle of the cross-section. Beam sections have an approximately central neutral axis despite only one plane of symmetry being applied. All column sections are symmetric about both axes and have a high or equal stiffness about one or two axes, respectively, due to the symmetric boundary conditions used in the optimisation process.

Further investigations are then conducted to improve the manufacturability and to characterise the compression behaviour of one of the best performing optimised sections. The improvement in manufacturability is done heuristically by keeping a similar cross-section philosophy whilst providing more uniform cross-section elements with constant thicknesses and curve radii. A final section is chosen after a comparison of the sections under the criteria of the second moment of area, the radius of gyration, and elastic buckling load under compression.

Stub column tests are carried out in FEA to finally determine the behaviour of the optimised aluminium sections under compression and to investigate the effectiveness of employing existing classification methods for these newly optimised profiles. It is found that 9 out of 10 of the sections tested behave as predicted by EC9.

This research will be further completed with the investigation of the resistance of the proposed sections under other local and global failure modes. More importantly, this research should constitute as a paradigm for future studies that focus on the development of sustainable and resilient lightweight structural engineering products (members and systems) through a combination of design optimisation methodologies - such as the one proposed in Fig. 4.

Acknowledgments

The authors would like to thank the Institution of Structural Engineers (IStructE) Research Grants for the continuous financial and technical support for the conduction of this novel project and the financial support of EPSRC (P/L022648/1). In addition, the contribution of Dr Pavlos Vatavalis, Chief Technical Officer of ETEM aluminium company is greatly acknowledged.

References

[1] M.P. Bendsoe, O. Sigmund, Topology Optimisation, Springer, 2004, https://www.springer.com/gb/book/9783540429920.
[2] U. Kirsch, Structural Optimisation - Fundamentals and Applications, Springer, 1993, pp. 1408–1415 https://www.springer.com/gb/book/9783540559191.
[3] Altair University, (2015). Practical Aspects of Structural Optimization. Altair Engineering, IncCivil-Comp Press, 2013 Proceedings of the Fourteenth International Conference on Civil, Structural and Environmental Engineering Computing, B.H.V. Topping and P. Iványi, (Editors), Civil-Comp Press, Stirlingshire, Scotland. ⟨http://altairuniversity.com/wp-content/uploads/2014/04/kingman-2013.pdf⟩.
[4] K. Anand, A. Misra, Topology optimization and structural analysis of simple column and short pressurized beams using optimality criterion approach in ANSYS, Int. Res. J. Eng. Technol. 2 (3) (2015) 1408–1415.
[5] M.P. Bendsoe, O. Sigmund, Topology Optimization, Theory, Methods and Applications, Springer, Berlin, 2013.
[6] B. Bochenek, K. Tajs-Zielińska, Minimal compliance topologies for maximal buckling load of columns, Struct. Multidiscip. Optim. 51 (5) (2015) 1149–1157.
[7] BSI, BS 5950-5:1998. Structural use of steelwork in building – Part 5: Code of Practice for Design of Cold Formed Thin Gauge Sections, British Standards Institute, London, 1998.
[8] BSI, BS EN 1993-1-1:2005: Eurocode 3: Design of Steel Structures - Part 1-1: General Rules and Rules for Buildings, British Standards Institute, London, 2005.
[9] BSI, BS EN 1991-1-1: Design of Aluminium Structure – Part 1-1: General Structural Rules, British Standards Institute, London, 2007.
[10] P.W. Christensen, A. Klarbring, An Introduction to Structural Optimization, Springer Science & Business Media, Springer, Netherlands, 2008https://www.springer.com/gb/book/9781402086656.
[11] J. Christensen, Topology Optimisation of Structures Exposed to Large (Non-linear) Deformations (Ph.D. thesis), Coventry University, UK, 2015https://curve.coventry.ac.uk/open/file/7c0729ce-e19c-414c-9542-c39527d54752/1/Christensen%202015.pdf.
[12] A. Crisan, V. Ungureanu, D. Dubina, Behaviour of cold-formed steel perforated sections in compression. Part 1 - Experimental investigations, Thin Walled Struct. 61 (2012) 86–96.
[13] J. Dwight, Aluminium Design and Construction, E & FN SPON, London, UK, 1999.
[14] R. Feng, B. Young, Experimental investigation of aluminum alloy stub columns with circular openings, Am. Soc. Civil Eng. 141 (11) (2015) 1–10.
[15] R. Gitter, Design of aluminium structures: selection of structural alloys. EUROCODES-Background and Applications, Brussels, Belgium, 2008.
[16] L. Grekavicius, J.A. Hughes, K.D. Tsavdaridis, E. Efthymiou, Novel morphologies of aluminium cross-sections through structural topology optimisation techniques, Key Eng. Mater. 710 (2016) 321–326.
[17] T. Höglund, Design of Members, TALAT Lecture 2301, 2009.
[18] T. Höglund, D. Kosteas, Special Design Issues, TALAT Lecture 2205, 1994.
[19] T. Höglund, P. Tindall, H. Gulvanessian, H. Gulvanessian (Ed.), Designers' Guide to Eurocode 9: Design of Aluminium Structures, ICE Publishing, 2012(Available from: ⟨http://www.icevirtuallibrary.com/doi/abs/10.1680/das.57371⟩, (Accesssed 2 March 2018)).
[20] X. Huang, Y.M. Xie, Evolutionary Topology Optimization of Continuum Structures: Methods and Applications, John Wiley & Sons, Ltd., 2010, https://onlinelibrary.wiley.com/doi/book/10.1002/9780470689486.
[21] H.G. Jøhansen, Structural Aluminium Materials. TALAT Lecture 2202, 1994.
[22] Y. Kim, T. Kim, Topology optimization of beam cross sections, Int. J. Solids Struct. 37 (3) (2000) 477–493.
[23] J.J. Kingman, K.D. Tsavdaridis, V.V. Toropov, Applications of topology optimisation in structural engineering: high-rise buildings & steel components, Jordan J. Civil. Eng. 9 (3) (2015) 335–357.
[24] Kobe Steel, Ltd. Yield Point and 0.2% Offset Yield Strength. [online] Kobelco-welding.jp, 2016. Available at: ⟨http://www.kobelco-welding.jp/education-center/abc/ABC_2005-04.html⟩. (accessed 3 May 2016).
[25] M. Liu, L. Zhang, P. Wang, Y. Chang, Buckling behaviours of section aluminium alloy columns under axial compression, Eng. Struct. 95 (2015) 127–137.
[26] F.M. Mazzolani, Aluminium Alloy Structures, Pitman, Boston, 1985.
[27] F.M. Mazzolani, Aluminium Alloy structures, CRC Press, London, 1994.
[28] F.M. Mazzolani, Aluminium Structural Design, CISM- International Center for Mechanical Sciences- Courses and Lectures No. 443, Springer-Verlag Wien, NewYork, Udine, Italy, 2003.
[29] J. Mennink, Cross-Sectional Stability of Aluminium Extrusions: Prediction of the Actual Local Buckling Behaviour, Technische Universiteit Eindhoven, Eindhoven, 2002, https://doi.org/10.6100/IR561443.
[30] M. Mesinger, R. Parral, C. Radlbeck, Optimization of extruded hollow aluminium profiles by applying genetic algorithms, in: L. Katgerman, F. Soetens (Eds.), New Frontiers in Light Metals, Proceedings of the 11th International Aluminium Conference INALCO, IOS Press, Inc., Delft, 2010, pp. 363–372.
[31] U. Muller, Introduction to Structural Aluminium Design, Whittles Publishing, Scotland, UK, 2011.
[32] D.J. Munk, A.V. Gareth, G.P. Steven, Topology and shape optimization methods using evolutionary algorithms: a review, Struct. Multidiscip. Optim. 52 (2015) 613–631.
[33] Non-Ferrous Extrusion. Aluminium information. [Online], 2012. Available from: ⟨http://www.non-ferrous.com/website/aluminum-information/⟩. (accessed 21 March 2018).
[34] G. Rozvany, A critical review of established methods of structural topology optimization, Struct. Multidiscip. Optim. 3 (37) (2008) 217–237.
[35] M.N. Su, B. Young, L. Gardner, Deformation-based design of aluminium alloy beams, Eng. Struct. 80 (2014) 339–349.
[36] M.N. Su, B. Young, L. Gardner, Classification of aluminium alloy cross-sections, Eng. Struct. 141 (2017) 29–40, https://doi.org/10.1016/j.engstruct.2017.03.007.
[37] K.D. Tsavdaridis, C. D'Mello Finite element investigation of perforated beams with different web opening configurations, in: Proceedings of the 6th International Conference on Advances is Steel Structures (ICASS 2009). 16–18 December 2009, Hong Kong, China, 2009, pp. 213–220.
[38] K.D. Tsavdaridis, C. D'Mello, Web buckling study of the behaviour and strength of perforated steel beams with different novel web opening shapes, J. Constr. Steel Res. 67 (10) (2011) 1605–1620.
[39] K.D. Tsavdaridis, C. D'Mello, Vierendeel bending study of perforated steel beams with various novel shapes of web openings, through non-linear finite element analyses, ASCE J. Struct. Eng. 138 (10) (2012) 1214–1230.
[40] K.D. Tsavdaridis, C. D'Mello, Optimisation of novel elliptically-based web opening shapes of perforated steel beams, J. Constr. Steel Res. 76 (2012) 39–53.
[41] K.D. Tsavdaridis, G. Galiatsatos, Assessment of cellular beams with transverse stiffeners and closely spaced web openings, Thin Walled Struct. 94 (2015) 636–650.
[42] K.D. Tsavdaridis, J.A. Hughes, L. Grekavicius, E. Efthymiou, Novel optimised structural aluminium cross-sections towards 3D printing, in: M. Meboldt, C. Klahn (Eds.), Industrializing Additive Manufacturing - Proceedings of Additive Manufacturing in Products and Applications - AMPA2017, 2018 Springer, Cham, 2017, pp. 34–46.
[43] K.D. Tsavdaridis, J. Kingman, V. Toropov, Application of structural topology optimisation to perforated steel beams, Comput. Struct. 158 (2015) 108–123.
[44] Y.M. Xie, G.P. Steven, Evolutionary Structural Optimization, Springer-Verlag, London, 1997https://www.springer.com/gb/book/9781447112501.
[45] R. Zuberi, Z. Zhengxing, L. Kai, Topological optimization of beam cross section by employing extrusion constraint, in: Proceedings of the 12th International Conference on Enhancement and Promotion of Computational Methods in Engineering and Science (EPMESC XII). Macau, 2009.
[46] R.H. Zuberi, Z. Zhengxing, L. Kai, Topological optimization of beam cross section by employing extrusion constraint, in: Proceedings of the ISCM II and EPMESC XII 1233(1) (2010) 964–969, 2010.